Efficient and Fast Wind Turbine MPPT Algorithm Using TS Fuzzy Logic and Optimal Relation Methods

David R. López-Flores, Pedro R. Acosta-Cano-de-los-Rios, Pedro R. Márquez-Gutierrez, José E. Acosta-Cano-de-los-Rios, Rogelio E. Baray-Arana, and Graciela Ramirez-Alonso

***Abstract*—This paper proposes an efficient and fast maximum power point tracking (MPPT) algorithm for a wind turbine (WT) connected to a battery bank via a permanent magnet synchronous generator, a three-phase diode rectifier, and a dc-dc boost converter. The algorithm is based on the Takagi-Sugeno (TS) fuzzy system and optimal relation methods and is called TS-MPPT. The fuzzy system computes the converter duty cycle using an input that combines the error and its rate of change. The error is the difference between the reference current computed from the optimal relation and the rectifier current. The methods used in the algorithm resulted in a five-rule TS fuzzy system, which contributed to a fast algorithm in terms of its total execution time (TET): 89.12 µs on the F28069M board. The TET attained enabled a synchronized operation of the algorithm with the converter switching frequency. Additionally, the results based on the processor-in-the-loop simulation approach show that the TS-MPPT algorithm achieves an effective MPP tracking process with an energy conversion efficiency of 99.43% and behaves properly when evaluated over the typical WT power curve. Furthermore, the effectiveness and performance of the proposed algorithm are demonstrated against others using the proportional-integral controller, the Mamdani fuzzy method, and a TS fuzzy model from the literature.**

Link to graphical and video abstracts, and to code: https://latamt.ieeer9.org/index.php/transactions/article/view/8727

***Index Terms*—Wind turbine system, MPPT algorithm, fuzzy logic, Takagi–Sugeno, optimal relation, F28069M board, PIL simulation.**

I. Introduction

The maximum power point tracking (MPPT) process plays a vital role in optimizing the energy conversion efficiency of renewable energy conversion systems (RECS) [1]. Since renewable energy sources are inherently variable, the maximum power point (MPP) of a RECS system based on either a wind turbine (WT) or a photovoltaic (PV) system varies. Therefore, an MPPT algorithm must be adopted in the RECS system to track its MPP with an acceptable energy conversion efficiency (ECE) [2], [3]. Due to their ease and practical implementation, perturbation and observation (P&O), hill climbing search (HCS), and incremental conductance (IC) are the most used conventional methods to design the MPPT algorithm. However, the main drawback of these methods is the power oscillation near the MPP operation, which negatively affects the energy conversion efficiency of the RECS system [4], [5]. To overcome this main drawback, several MPPT algorithms based on modern computational intelligence methods have been proposed, including fuzzy logic systems based on the Mamdani or Takagi-Sugeno (TS) inference models [5]–[7]. Some of the closest literature in this regard is the MPPT algorithm discussed in [8], which achieved an ECE of 97.44%. This algorithm was designed based on the TS fuzzy inference model with 25 rules and the power-voltage (P-V) curve methods. Its primary control objective was to track the MPP of a RECS system consisting of a PV emulator, a dc-dc converter, and a resistive load. The inputs to the TS fuzzy system were the slope of the P-V curve, S, and its rate of change, ΔS. The system output was the change of the duty cycle signal Δd to the dc-dc converter. The work in [9] presented an MPPT algorithm for a RECS system comprised of a WT connected to the electrical grid via a permanent magnet synchronous generator (PMSG), a controlled rectifier, and a dc-ac inverter. The algorithm was designed based on a dq-axis cascade control scheme using the TS fuzzy and optimal power (OP) methods to control the rectifier. In order to maximize the delivered real power to the grid, the TS fuzzy system with 25 rules used in the q-axis reference frame was optimized using the whale optimization algorithm (WOA). The inputs to the TS fuzzy system were the error of the WT optimal power e, the errors of the PMSG dq-axis currents e_{id} and e_{iq}, respectively, as well as their rate of changes. The fuzzy system outputs were the PMSG reference values of the q-axis current $i_{q,ref}$ and the dq-axis voltages $v_{d,ref}$ and $v_{q,ref}$, respectively.

Table I summarizes the design details of the previously mentioned MPPT algorithms [8], [9], and other similar algorithms [10]–[13]. These details include the RECS system type, the methods used to design the MPPT algorithm, the inputs/outputs utilized in the TS fuzzy systems, and the number of rules employed. In addition to the studies presented in Table 1, the works described in [14]–[18], also used the TS fuzzy theory for modeling RECS systems in state-space representations. This modeling was achieved by combining local linear dynamic subsystems using *if-then* fuzzy rules.

D. R. López-Flores, P. R. Acosta-Cano-de-los-Rios, P. R. Márquez-Gutierrez, J. E. Acosta-Cano-de-los-Rios, and R. E. Baray-Arana are with Tecnológico Nacional de México / IT de Chihuahua, Ave. Tecnológico 2909 Chihuahua, México (emails: david.lf@chihuahua.tecnm.mx, pacosta@itchihuahua.edu.mx, pedro.mg@chihuahua.tecnm.mx, jose.ac@chihuahua.tecnm.mx, and rogelio.ba@chihuahua.tecnm.mx).

G. Ramírez-Alonso is with Universidad Autónoma de Chihuahua / Facultad de Ingeniería, Circuito Número I s/n, Chihuahua, México (email: galonso@uach.mx).

TABLE I
SUMMARY OF THE LITERATURE SHOWING IMPLEMENTATION DETAILS OF MPPT ALGORITHMS USING THE TS FUZZY SYSTEM WITH OTHER METHODS

Ref.	RECS	MPPT Methods	[Inputs / Ouputs]	Rules
[8]	PV	TS fuzzy-P-V	[S, ΔS / Δd]	25
[9]	WT	TS fuzzy[1]-OP	Multiples[2]	25[3]
[10]	WT	TS fuzzy[4]	[e, Δe / β][5]	5
[11]	PV	TS fuzzy-P-V	[ΔP, (ΔP/Δd) / Δd][6]	25
[12]	PV	TS fuzzy-IC	[S, ΔS / Δd]	25
[13]	PV	TS fuzzy-P-V	Multiples[7]	18

[1] It was optimized with WOA.
[2] Three TS fuzzy systems: [e, Δe / $i_{q,ref}$], [e_{iq}, Δe_{iq} / $v_{q,ref}$], and [e_{id}, Δe_{id} / $v_{d,ref}$].
[3] For the TS fuzzy systems used in the q-axis reference frame.
[4] It was optimized using an advanced intelligent genetic algorithm (AIGA) to limit the WT power.
[5] [WT speed error and its rate of change / WT blade pitch angle].
[6] [PV power change and its rate of change/ PV duty cycle change].
[7] [S, ΔS, V, $\Delta d(k-1)$ / Δd]; V stands for the PV voltage.

Subsequently, using these representations and to effectively track the MPP of the RECS systems, feedback gains for the MPPT algorithm based on the TS fuzzy method were designed using suitable techniques such as parallel distributed compensation (PDC) and linear matrix inequality (LMI).

The methods presented in Table I and those based on the TS fuzzy modeling [14]–[18] lead to a suitable design and performance of the MPPT algorithms for effectively tracking the MPP of the RECS systems. However, it can be seen from Table I that, except for [10], a high number of rules is associated with TS fuzzy systems that analyze more than one input. Besides, the number of rules of the MPPT algorithms based on TS fuzzy modeling increases with respect to RECS system state variables. Many rules negatively affect the total execution time of the MPPT algorithm and its synchronization process with the operation frequency of the power converters of the RECS systems. Furthermore, designing feedback gains through PDC and LMI techniques, as well as state-space representations, requires a detailed mathematical model of the RECS systems. Moreover, the performance of the outlined MPPT algorithms dealing with WT systems was not assessed across the operating regions of the typical WT power curve. These operating regions ensure efficient and safe operation of the WT system across an entire range of wind speeds. Also, the presented MPPT algorithms have not integrated a single combined input of both the error and its rate of change within the TS fuzzy system to compute the output signal. This integration can positively impact the rule number of the TS fuzzy system and significantly enhance the MPP tracking process of the RECS system when it is subjected to sudden fluctuations of the renewable energy. Finally, with the exception of [8], [16], and [18], the performance of the analyzed MPPT algorithms was not evaluated using the energy conversion efficiency criterion of the RECS system. It is also worth noting that none of the presented algorithms reported its total execution time (TET) via simulators or hardware boards.

Given this background, this paper presents a wind turbine MPPT algorithm called TS-MPPT based on a TS fuzzy system and optimal relation methods. The WT is connected to a battery bank via a PMSG generator, a three-phase diode rectifier, and a dc-dc boost converter. The fuzzy system computes the duty cycle signal d to the dc-dc converter using a combined input consisting of the error e and its rate of change Δe. The e signal is the difference between the reference current i_{ref} and the rectifier current i_o. The i_{ref} value is computed from the optimal relation, which leads to the MPP of the WT system. The methods used to design the TS-MPPT algorithm lead to the following main contributions:

i. A five-rule TS fuzzy system designed without relying on complex mathematical models.
ii. An effective MPP tracking process with an ECE of 99.43%, even if the WT system is subject to sudden fluctuations of the renewable energy.
iii. The proposed algorithm performs properly when assessed across the typical WT power curve. This performance and the effective MPPT process are demonstrated in comparison to other MPPT algorithms based on the proportional-integral controller (PI-MPPT), the Mamdani fuzzy method (MA-MPPT), and a TS fuzzy model from [8] (Oubella-MPPT). The comparison is carried out using the processor-in-the-loop (PIL) simulation approach.
iv. The TET of our proposed algorithm, measured in the F28069M board, is 89.12 μs, which enables a synchronization of the algorithm with the switching frequency of the dc-dc boost converter of the WT system. This TET is approximately 31 and 1.3 times faster than the MA-MPPT and Oubella-MPPT algorithms, respectively.

The remaining sections are organized as follows. First, a description of the WT system and the proposed TS-MPPT algorithm are presented in Section II. Then, Section III presents the PIL simulation results and discussions aimed to demonstrate the performance and effectiveness of the proposed algorithm versus other ones based on the proportional-integral (PI) controller and the Mamdani fuzzy method. Additionally, the hardware implementation details of the proposed algorithm on the F28069M board, used for measuring the total execution time, are described in Section III. Finally, the conclusions are given in Section IV.

II. THE PROPOSED TS-MPPT ALGORITHM

This section describes the WT system and presents the methodology used to design the proposed TS-MPPT algorithm.

A. WT System Description

Fig. 1 shows the block diagram of the wind turbine system used in this paper. The WT converts the kinetic energy of the wind into mechanical power P_m. Then, the PMSG generator, along with the three-phase diode rectifier, converts this P_m power into dc electrical levels of current i_o and voltage v_o. The dc-dc boost converter adjusts the i_o and v_o levels via the d signal to charge the battery bank at an optimal current value i_{opt} corresponding to the MPP of the wind turbine. The d signal is calculated by the proposed TS-MPPT algorithm based on the wind speed V_w and i_o values. The methodology used to design the TS-MPPT algorithm is presented in the following section.

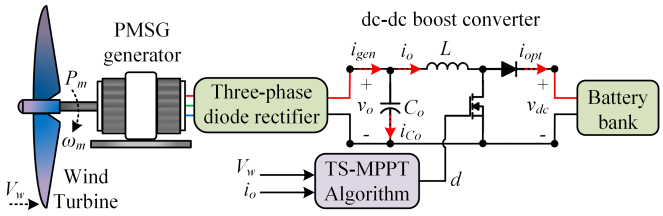

Fig. 1. Block diagram of the wind turbine system.

B. Proposed TS-MPPT Algorithm Design Methodology

The WT system in Fig. 1 can be studied using the equivalent circuit depicted in Fig. 2. The WT, along with both the PMSG generator and the rectifier, as well as the battery bank, are considered ideal dc voltage sources represented by the symbols v_o and v_{dc}, respectively. Dynamics and power losses are not considered. The dc-dc boost converter is considered a controlled current source, requiring activation by the d signal to adjust the levels of v_o and i_o for charging the battery bank at an optimal current value of i_{opt}. Therefore, an MPPT algorithm is necessary to compute the d signal to ensure the appropriate activation of the controlled source.

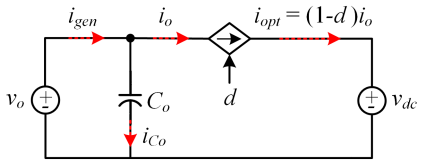

Fig. 2. Equivalent circuit of WT system.

The d signal can be derived by applying Kirchhoff's current law in Fig. 2, as shown below:

$$C_o \frac{dv_o}{dt} = (i_{gen} - i_o) \tag{1}$$

where i_{gen} represents the rectifier current. Eq. (1) can be rewritten as follows during steady-state conditions:

$$i_{gen} = i_o = \frac{i_{opt}}{1-d} \tag{2}$$

where i_o in Eq. (2) can be considered the rectifier current. In addition, the value of the d signal, which ensures that the battery bank is charged at an i_{opt} value, can be obtained via a controller that processes the deviations of the i_o current regarding its reference value i_{ref}, as follows:

$$d = Controller \cdot (i_{ref} - i_o) \tag{3}$$

In this work, the i_{ref} value in Eq. (3) is computed from the optimal relation method, which is explained below. Considering a fixed WT blade pitch angle, the mechanical power generated by the wind turbine, P_m, can be expressed as:

$$P_m = 0.5\rho\pi R^2 V_w^3 C_p(\lambda) \tag{4}$$

where ρ, R, C_p, and λ stand for the air density, the WT rotor radius, the power coefficient, and the tip speed ratio, respectively.

In this work the C_p coefficient is a nonlinear function that varies with the λ ratio, defined as:

$$C_p = c_1\lambda^7 + c_2\lambda^6 + c_3\lambda^5 + c_4\lambda^4 + c_5\lambda^3 + c_6\lambda^2 + c_7\lambda + c_8 \tag{5}$$

$$\lambda = \frac{\omega_m R}{V_w} \tag{6}$$

where c_1 to c_8 are constant values, and ω_m is the rotational speed.

Considering the parameters in Table IV from the Appendix and using Eqs. (5) and (6), the typical C_p versus λ curve is shown in Fig. 3. Note that there is an optimal power coefficient value $C_{p,opt}$ of 0.3493, which corresponds to an optimal tip speed ratio λ_{opt} of 5.9. These optimal values are fixed for a given WT design.

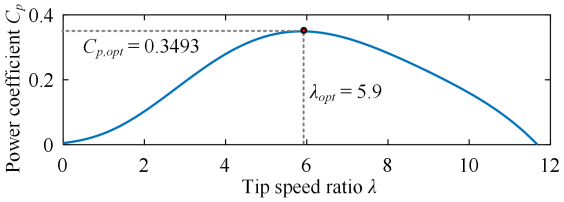

Fig. 3. Typical power coefficient curve.

Substituting the optimal C_p coefficient and λ ratio depicted in Fig. 3 into Eqs. (4) and (6), the optimal mechanical power can be expressed as a function of the optimal rotational speed, defined as:

$$P_{m,opt} = 0.5\rho\pi R^5 \frac{\omega_{m,opt}^3}{\lambda_{opt}^3} C_{p,opt} = K_{opt}\omega_{m,opt}^3 \tag{7}$$

The electrical power leading to the MPP of the WT system can be associated with Eq. (7) by considering the efficiency η of the PMSG generator and the rectifier, as described below:

$$\eta K_{opt}\omega_{m,opt}^3 = i_{o,ref} v_o \tag{8}$$

Equations (7) and (8), and Fig. 3, show that there is an optimal relationship at the MPPT for a given wind turbine system design, defined as:

$$i_{o,ref} = k_1\omega_{m,opt}^3 + k_2\omega_{m,opt}^2 + k_3\omega_{m,opt} + k_4 \tag{9}$$

where k_1 to k_4 are constants, and as previously mentioned, $i_{o,ref}$ and $\omega_{m,opt}$ are the reference current and the optimal rotational speed when the WT system is at MPP, respectively.

Considering the parameters of Tables IV and V from the Appendix, the $i_{o,ref}$ versus $\omega_{m,opt}$ characteristics of the WT system depicted in Fig. 3 at different wind speeds (V_{w1} =3 m/s to V_{w14} =16 m/s) are shown in Fig. 4. The blue nonlinear line is the optimal relation between $i_{o,ref}$ and $\omega_{m,opt}$, which can be approximated using Eq. (9) with $k_1 = 0.0025$, $k_2 = -0.072$, $k_3 = 1.36$, and $k_4 = -5.68$. Therefore, Eq. (9) can be utilized to compute $i_{o,ref}$, or record a lookup table based on Fig. 4 with data points for $i_{o,ref}$ and the corresponding $\omega_{m,opt}$ values. Then, using the interpolation procedure in the recorded table, it is possible to compute the value of $i_{o,ref}$. In this work, a recorded table was used.

As previously mentioned, the controller in Eq. (3) calculates the d signal based on the deviation of the i_o current from $i_{o,ref}$, achieving the MPP of the WT system. In contrast to the MPPT algorithms presented in [8]–[18], this work uses

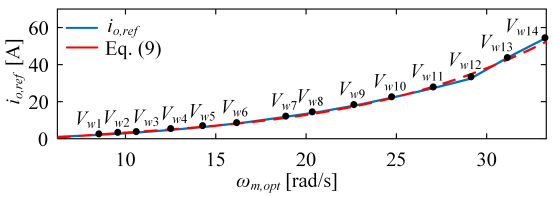

Fig. 4. Nonlinear optimal relation curve of $i_{o,ref}$ versus $\omega_{m,opt}$.

a TS fuzzy system as the controller to compute the d signal based on a combined input consisting of the e and Δe signals. The mathematical model of the TS fuzzy system is designed based on the following premise: when the combined input value $(e+\Delta e)$ is considerable and exhibits a specific polarity, the rate of change of the duty cycle Δd must be directly proportional to the magnitude of the combined input while maintaining that polarity. This combined input contains crucial information about the magnitude of the steady-state errors due to e and the direction and magnitude of the transient states due to Δe. When the TS fuzzy system processes this information, it inherently results in the computation of changes in the direction and magnitude of the d-signal for the dc-dc converter, reducing overshoot and accurately capturing sudden fluctuations of the renewable source. A detailed diagram of the proposed TS-MPPT algorithm is presented in Fig. 5. This TS-MPPT algorithm is based on Eq. (3) and the lookup table obtained from Fig. 4. The following section describes the details of this TS-MPPT algorithm.

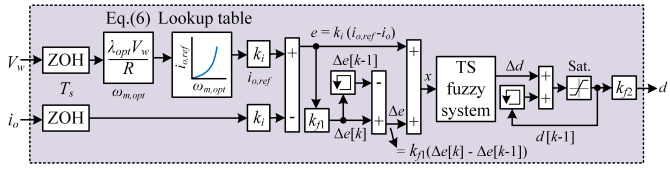

Fig. 5. The proposed TS-MPPT algorithm connection diagram.

According to Fig. 5, the V_w and i_o measurements are discretized via the zero-order hold (ZOH) method with a sampling time rate set by $T_s = 200$ μS. Eq. (6) processes the discrete V_w measurement to determine the $\omega_{m,opt}$ value. Next, the lookup table estimates $i_{o,ref}$ based on the $\omega_{m,opt}$ value. The k_i blocks attenuate the $i_{o,ref}$ value and the discrete i_o measurement before determining the e and Δe signals as depicted in Fig. 5. The TS fuzzy system then analyzes the behavior of the combined input $x = e + \Delta e$ to compute the Δd signal. Finally, the computation of the d signal for the dc-dc converter involves multiplying the constant k_{f2} by the sum of the Δd signal and the previous value of the duty cycle signal $d[K-1]$. The constants k_i, k_{f1}, k_{f2} are set to $1/22$, 200, and 9000, respectively, for normalization purposes. The $Sat.$ block avoids saturation operating regions of the dc-dc converter. The lookup table considers a typical WT power curve to trigger the cut-in wind speed at 3 m/s, initiate the MPPT process between 3 m/s and 16 m/s (determined based on the optimal relationship shown in Fig. 4), maintain the rated power from 16 m/s to 17 m/s, and activate the cut-out wind speed above 17 m/s. The detailed design of the TS fuzzy system is described below.

The TS fuzzy system shown in Fig. 5 consists of an input fuzzification stage, an inference method, and an output stage [8]. The trapezoidal and generalized bell-shaped membership functions illustrated in Fig. 6 are utilized to define the fuzzy sets that represent the input to the fuzzy system. These membership functions aid in providing a smoother control surface to minimize sudden changes in the d signal. The fuzzy sets for the combined input $x = e + \Delta e$ are represented by the linguistic terms A_1, A_2, A_3, A_4, and A_5, which stand for negative big, negative, zero, positive, and positive big, respectively.

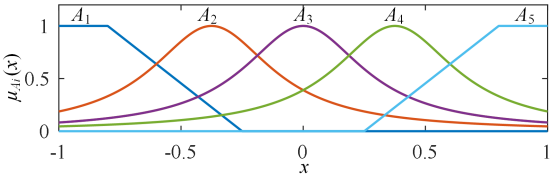

Fig. 6. Membership functions plots for the combined input x.

The output of the fuzzy system is defined by Eqs. (10)-(14).

$$\Delta d_1(x) = -0.017 \tag{10}$$

$$\Delta d_2(x) = 0.0023x - 0.0092 \tag{11}$$

$$\Delta d_3(x) = 0.00046x \tag{12}$$

$$\Delta d_4(x) = 0.0023x + 0.0092 \tag{13}$$

$$\Delta d_5(x) = 0.017 \tag{14}$$

The set of fuzzy rules used in our TS fuzzy system is presented in Table II. These rules are defined based on the premise previously presented as prior knowledge in combination with the fuzzy sets shown in Fig. 6 and Eqs. (10)-(14). These rules are interpreted through the following deductive structure:

$$\text{If } x \text{ is } A_i, \text{ then } \Delta d \text{ is } \Delta d_i(x) \tag{15}$$

where i = 1, 2,..., 5.

TABLE II
THE FUZZY RULE SET FOR THE TS FUZZY SYSTEM

x	Δd
A_1	$\Delta d_1(x)$
A_2	$\Delta d_2(x)$
A_3	$\Delta d_3(x)$
A_4	$\Delta d_3(x)$
A_5	$\Delta d_4(x)$

Fig. 7 shows the control surface output of the fuzzy system. This surface is a graphical representation depicting the relationship between the Δd signal and x.

According to Fig. 5 and the control surface shown in Fig. 7, the final computation of the d signal is obtained as follows:

$$d = \frac{\sum_{i=1}^{5} \Delta d_i(x)\mu_{A_i}(x)}{\sum_{i=1}^{5} \mu_{A_i}(x)} + d[k-1] \tag{16}$$

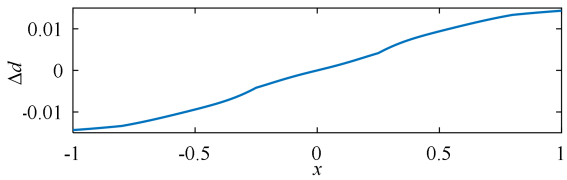

Fig. 7. Control surface output of the TS fuzzy system.

From the deductive structure (15), $\Delta d_i(x)$ represents the output level of each rule R_i, and $\mu_{A_i}(x)$ stands for the degree of activation of each R_i.

The approach used to design Eqs. (10)-(14) and the set of fuzzy rules presented in Table II is described below. First, a five-rule Mamdani fuzzy system was designed considering the same linguistic terms shown in Fig. 6 for the input x and output Δd. Assuming a maximum execution time of 100 μs for the fuzzy system, the domain of x was set according to Fig. 6, while for Δd, it was set from -0.02 to 0.02. Then, the inference method of the Mamdani system was established with a similar deductive structure derived from Eq. (15) (e.g., if x is A_1, then Δd is A_1), generating a control surface output. Using this control surface, five functions (Eqs. (10)-(14)) and five fuzzy rules were designed to represent this control surface, but now, using a TS fuzzy system. For example, the first TS fuzzy rule was established by considering the range of x associated with the linguistic term A_1, where the first function (Eq. (10)) accurately maps to the control surface obtained with the Mamdani fuzzy system. This TS fuzzy rule can be summarized as follows: if x is A_1, then Δd is $\Delta d_1(x)$. The TS fuzzy rule set presented in Table II was derived through this fuzzy reasoning process.

III. Simulation, Discussions and F28069M Algorithm Implementation

As described in a previous study [19], the PIL simulation approach is adopted for this work. It is done by considering, in Fig. 1, an inductor $L = 80$ mH, a capacitor $C_o = 470$ μH, and $v_{dc} = 500$ V, along with the parameters listed in Tables IV-V from the Appendix. A wind profile consisting of steps and fluctuations is used to evaluate the MPPT process using the proposed TS-MPPT algorithm. Additionally, wind steps are used to evaluate the performance of the TS-MPPT algorithm across the typical WT power curve. These evaluations involve comparing the TS-MPPT algorithm with the PI-MPPT, MA-MPPT, and Oubella-MPPT algorithms, which are implemented according to Eq. (3). Using the Bode stability criteria [20], the PI controller was tuned at a fixed operating point of $V_w = 12$ m/s to maintain a phase margin of 78.8° at 58.72 Hz and a gain margin of 30.5 dB at 2.5 kHz in the WT system. The implementation details of the MA-MPPT and Oubella-MPPT algorithms are shown in Table III.

According to the previously mentioned PIL simulation parameter settings, Fig. 8 shows the result comparisons between the proposed TS-MPPT algorithm and those based on PI-MPPT, Oubella-MPPT, and MA-MPPT. Fig. 8 (a) depicts the control performance of i_o deviations regarding the $i_{o,ref}$ of

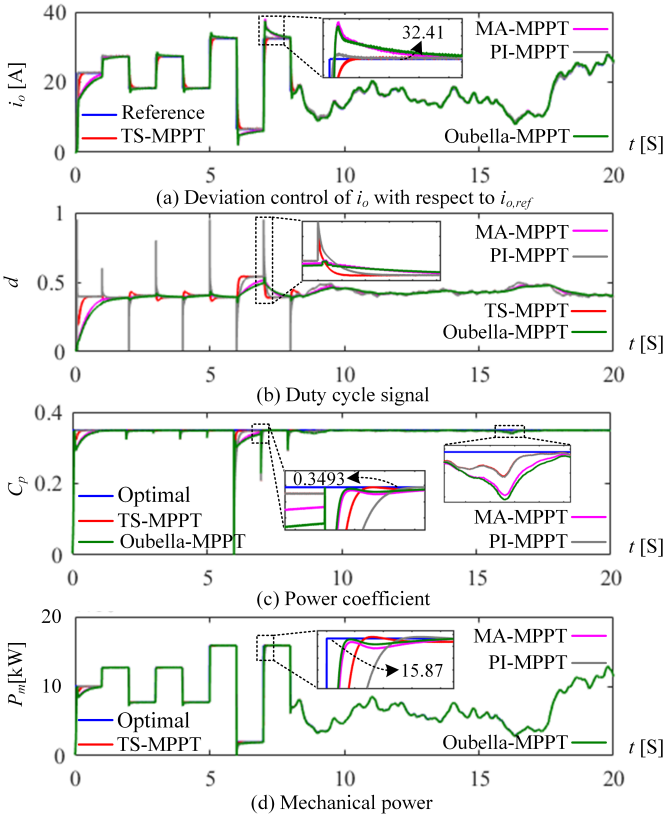

Fig. 8. Performance of the proposed MPPT algorithm compared to others based on PI controller, TS fuzzy model of [8], and Mamdani fuzzy method using the PIL simulator.

the four algorithms. At $t = 7$ s, the proposed algorithm minimizes deviations without overshoots, in comparison to the MA-MPPT, Oubella-MPPT, and PI-MPPT algorithms. This performance consistency extends to the step reference regions, enabling better capture of wind energy even during sudden fluctuations in renewable energy. The effective control of the i_o deviation obtained with the proposed algorithm is attributed to the capacity of the TS fuzzy system to rapidly compute the necessary initial and transient responses of the d signal for the dc-dc converter, as demonstrated in Fig. 8 (b) over the time evolution, especially at $t = 7$ s. The capacity of the TS fuzzy system is attributed to its mathematical model, established on the basis of Fig. 5, which allows the estimation of the Δd signal without accumulative effects. This property implies that the estimation of the Δd signal doesn't rely on its previous value, which inherently extends to the computation of the d signal. The power coefficient and mechanical power obtained by the proposed TS-MPPT algorithm, in comparison with the PI-MPPT, Oubella-MPPT, and MA-MPPT algorithms, are illustrated in Fig. 8 (c) and (d), respectively. At $t = 7$ s, it can be observed that the proposed algorithm achieves the best performance by maintaining less deviations of C_p and P_m from their optimal values compared to the other algorithms. This performance inherently extends over the evolution of the C_p coefficient and P_m power over time, especially within the step regions. The effective performance of the TS-MPPT algorithm is due to its capacity to suitably compute the d

signal, as previously discussed, leading to enhanced control of the i_o deviations from its reference value. Applying the energy conversion efficiency criterion defined in Eq. (17) to the P_m power of the proposed TS-MPPT algorithm, an efficiency of 99.43% is obtained. This acceptable result is attributed to the improved handling of sudden fluctuations of the renewable energy by the proposed algorithm, as previously demonstrated in Fig. 8.

$$n_{mppt} = \frac{\int_0^t P_m \, dt}{\int_0^t P_{m,opt} \, dt} \tag{17}$$

Fig. 9 demonstrates the effectiveness of the proposed TS-MPPT algorithm across the WT power curve compared to the PI-MPPT, Oubella-MPPT, and MA-MPPT algorithms. In Fig. 9 (a), during the interval MPPT process 1, V_w speed varies from 12 to 16 m/s, and all algorithms appropriately track the i_o reference values to minimize i_o deviations. Consequently, deviations of the P_m power concerning its optimal value are minimized, as shown in Fig. 9 (b). Moreover, within the rated power (RP) interval, the lookup table depicted in Fig. 5 computes the necessary i_o reference values to limit the P_m value at the rated power. During this interval, the P_m power of all algorithms deviates from its optimal value (27.42 kW), as depicted in Fig. 9 (b), aiming to mitigate potential electrical or structural damage to the overall system. Beyond the cut-out wind speed, when $V_w > 17$ m/s, the i_o and P_m values of all algorithms drop to zero from 5 to 7 s, as indicated in Figs. 9 (a) and (b), respectively. It aids in preventing damage to the overall system due to high wind speeds. After the cut-out wind speed, V_w changes from 18 m/s to 14 m/s, and the MPPT process of the WT system is activated again. Subsequently, V_w speed drops to 2 m/s from 9 to 11 s, and the WT system shuts down. Next, the cut-in wind speed of the WT system is triggered. Note in Figs. 9 (a) and (b) that during the intervals of MPPT process 2 and 3, unlike the proposed TS-MPPT, Oubella-MPPT, and MA-MPPT algorithms, the PI MPPT algorithm neither tracks the i_o reference values nor returns to the MPPT process ($P_m \approx P_{m,opt}$), respectively. This behavior is due to the accumulative effect associated with the integral action of the PI controller.

The implementation of the proposed TS-MPPT algorithm on the F28069M board for measuring the total execution time (TET) is depicted in Fig. 10. According to the simulator environment, two methods were used: block prioritization (BP) and code execution profiling (CEP). The first one consists of specifying the block order of execution relative to other blocks, illustrated by the red letters in Fig. 10. Once the algorithm is downloaded to the F28069M board, the order of execution starts according to the block prioritization. It means the algorithm is executed in the following order: first set high the general purpose input/output (GPIO) 32, wind speed measurement, current measurement, the conversions, Eq. (6) along lookup table for compute the $i_{o,ref}$ value, TS fuzzy system for compute the d signal, updating of the pulse-width modulation (PWM), and finally is set low the GPIO 32. According to this execution order, the GPIO 32 high time is measured by an oscilloscope, which corresponds

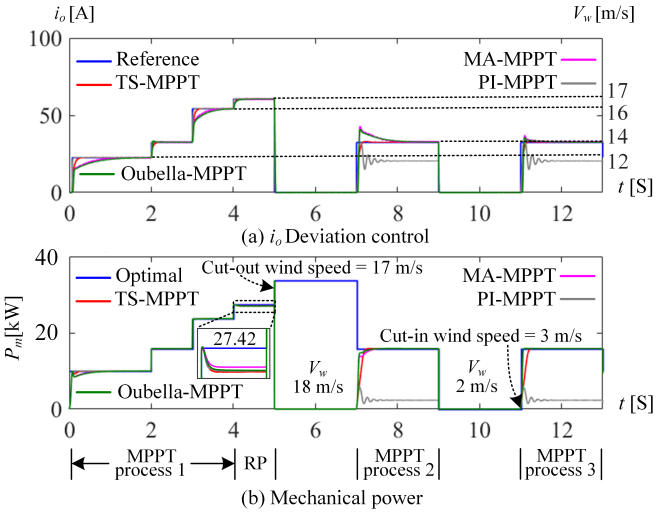

Fig. 9. Effectiveness of the proposed TS-MPPT algorithm across the WT power curve compared to others based on PI controller, TS fuzzy model of [8], and Mamdani fuzzy method.

approximately to the TET of the algorithm. In the second method, code execution profiling involves downloading the algorithm onto the F28069M board. Then, by entering the command *codertarget.profile.getData('algorithm name')* in the command window of the simulator, a CEP report containing the TET of the algorithm can be uploaded to the workspace [21]. Extending the methods presented above to the MA-MPPT, Oubella-MPPT, and PI-MPPT algorithms, Table III shows the TET of all algorithms. Considering the mid-range, note that the proposed TS-MPPT algorithm is approximately 31 and 1.3 times faster than the MA-MPPT and Oubella-MPPT, respectively, and roughly 2.5 times slower than the PI-MPPT algorithm. In addition, the proposed TS-MPPT algorithm, compared with the MA-MPPT algorithm, can enable synchronous implementation with the switching frequency of the dc-dc converter, whose maximum value can be up to 10 kHz. This work utilized a frequency of 5 kHz, and the TS-MPPT and PI-MPPT algorithms were synchronized with this frequency.

TABLE III
THE TET OF ALL ALGORITHMS BASED ON THE BLOCK PRIORITIZATION AND CODE EXECUTION PROFILING METHODS

Algorithm	TET of BP	Mid-range	TET of CEP
PI-MPPT	32 μs	34.95 μs	37.90 μs
TS-MPPT	84 μs	89.12 μs	94.25 μs
Oubella-MPPT[1]	104 μs	115.49 μs	126.98 μs
MA-MPPT[2]	2.8 ms	2.825 ms	2.850 ms

[1] Implementation details: two inputs (e, Δe), one output (Δd), triangular and trapezoidal membership functions to represent the inputs, constant functions to represent the output, a set of 25 fuzzy rules, and the TS inference method was used for defuzzifying the output of the fuzzy system [8].

[2] Implementation details: two inputs (e, Δe), one output (Δd), triangular membership functions to represent the inputs/output, a set of 25 fuzzy rules, and the centroid method was used for defuzzifying the output of the fuzzy system.

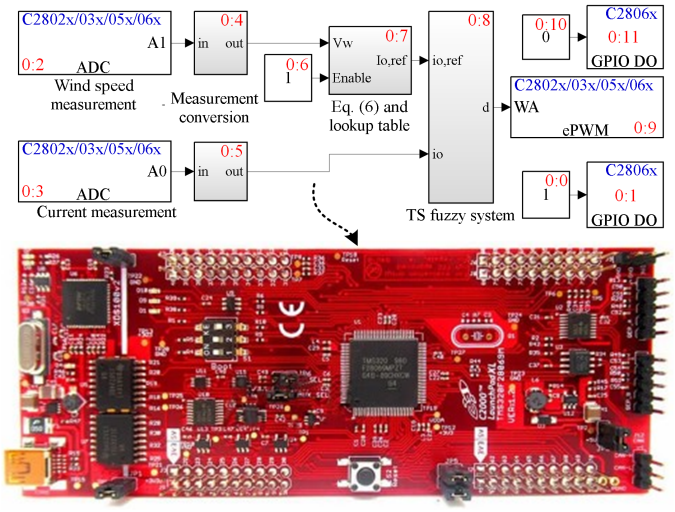

Fig. 10. Implementation of the proposed algorithm on the F28069M board for total execution time measurement.

According to the previous findings, the proposed TS-MPPT algorithm effectively maintains the MPP of the WT turbine system while ensuring acceptable energy conversion efficiency. Moreover, when assessed across the typical WT power curve, the proposed algorithm demonstrates appropriate performance. Additionally, the methodology used to design the TS-MPPT algorithm, which avoids dependency on complex mathematical models, resulted in an algorithm with a total execution time of 89.12 μs, measured in the F28069M board, and synchronized with the switching frequency of the dc-dc boost converter of the WT system.

The proposed TS-MPPT algorithm offers inherent advantages, including its effectiveness against sudden fluctuations in renewable energy and stable performance along the WT power curve. These advantages are crucial in optimizing the energy conversion efficiency of the WT system in challenging environments. In this regard, the algorithm could be adapted by including sub-modes of operating points within the MPPT process region. This adaptation could improve the energy conversion efficiency of the WT system when exposed to wind slowdown and wake effects, which are common in wind farms [22], [23].

IV. Conclusions

An MPPT algorithm for a WT system, designed via the TS fuzzy logic and optimal relation methods, is proposed in this paper. The methodology used to design the proposed algorithm avoids relying on complex mathematical models. Compared with the PI-MPPT, Oubella-MPPT, and MA-MPPT algorithms, the PIL simulation results demonstrate that the proposed algorithm improves the i_o tracking process without overshooting. This is due to the effective ability of the TS fuzzy system to fast compute the Δd signal without accumulative effects. The i_o deviations obtained with the proposed algorithm result in less deviations of the C_p coefficient and the P_m power of the WT turbine from their optimal values compared to the other algorithms. These results positively impact the energy conversion efficiency of the WT system, achieving a value of 99.43%. This efficiency is maintained even though the WT system is subjected to sudden fluctuations in renewable energy. In addition, the TET obtained with the proposed algorithm is 89.12 μs, which allows the synchronization of the algorithm with the switching frequency of the dc-dc boost converter of the WT system. This TET is approximately 31 and 1.3 times faster than the MA-MPPT and Oubella-MPPT algorithms, respectively.

The design methodology used in the proposed TS-MPPT algorithm can be extended to other REC systems, and the TS fuzzy system model can be adapted as the controller in other control systems. This extension or adaptation would inherit the same contributions claimed in this paper.

References

[1] M. J. Khan, L. Mathew, M. A. Alotaibi, H. Malik, and M. E. Nassar, "Fuzzy-logic-based comparative analysis of different maximum power point tracking controllers for hybrid renewal energy systems," *Mathematics (Basel)*, vol. 10, no. 3, pp. 529–, 2022. https://doi.org/10.3390/math10030529.

[2] M. A. Morales Caporal, J. d. J. Rangel Magdaleno, I. Cruz Vega, and R. Morales Caporal, "Improved grid-photovoltaic system based on variable-step mppt, predictive control, and active/reactive control," *IEEE Latin America Transactions*, vol. 15, no. 11, pp. 2064–2070, 2017. DOI:10.1109/TLA.2017.8070409.

[3] A. A. Salem, N. A. N. Aldin, A. M. Azmy, and W. S. E. Abdellatif, "Implementation and validation of an adaptive fuzzy logic controller for mppt of pmsg-based wind turbines," *IEEE Access*, vol. 9, pp. 165690–165707, 2021. DOI:10.1109/ACCESS.2021.3134947.

[4] R. B. Bollipo, S. Mikkili, and P. K. Bonthagorla, "Hybrid, optimal, intelligent and classical pv mppt techniques: A review," *CSEE Journal of Power and Energy Systems*, vol. 7, no. 1, pp. 9–33, 2021. DOI:10.17775/CSEEJPES.2019.02720.

[5] C. V. Govinda, S. V. Udhay, C. Rani, Y. Wang, and K. Busawon, "A review on various mppt techniques for wind energy conversion system," in *2018 International Conference on Computation of Power, Energy, Information and Communication (ICCPEIC)*, pp. 310–326, 2018. DOI:10.1109/ICCPEIC.2018.8525219.

[6] M. Mao, L. Cui, Q. Zhang, K. Guo, L. Zhou, and H. Huang, "Classification and summarization of solar photovoltaic mppt techniques: A review based on traditional and intelligent control strategies," *Energy reports*, vol. 6, pp. 1312–1327, 2020. https://doi.org/10.1016/j.egyr.2020.05.013.

[7] X. C. Le, M. Q. Duong, and K. H. Le, "Review of the modern maximum power tracking algorithms for permanent magnet synchronous generator of wind power conversion systems," *Energies (Basel)*, vol. 16, no. 1, pp. 402–, 2023. https://doi.org/10.3390/en16010402.

[8] M. Oubella, M. Ajaampun, and B. Bouachrine, "Low cost microcontroller implementation of takagi–sugeno fuzzy mppt controller for photovoltaic systems," *International Journal of Electrical and Computer Engineering Systems*, vol. 13, no. 10, pp. 971–981, 2022. https://doi.org/10.32985/ijeces.13.10.12.

[9] M. H. Qais, H. M. Hasanien, and S. Alghuwainem, "Enhanced whale optimization algorithm for maximum power point tracking of variable-speed wind generators," *Applied Soft Computing*, vol. 86, p. 105937, 2020. https://doi.org/10.1016/j.asoc.2019.105937.

[10] Z. Civelek, "Optimization of fuzzy logic (takagi-sugeno) blade pitch angle controller in wind turbines by genetic algorithm," *Engineering Science and Technology, an International Journal*, vol. 23, no. 1, pp. 1–9, 2020. https://doi.org/10.1016/j.jestch.2019.04.010.

[11] L. L. Wang, "Mppt control for photovoltaic system based on t-s fuzzy reasoning," in *2015 5th International Conference on Electric Utility Deregulation and Restructuring and Power Technologies (DRPT)*, pp. 1976–1980, 2015. DOI: 10.1109/DRPT.2015.7432562.

[12] H. Abbes, H. Abid, and K. Loukil, "An improved mppt incremental conductance algorithm using ts fuzzy system for photovoltaic panel," *International journal of renewable energy research*, vol. 5, no. 1, pp. 160–167, 2015. https://doi.org/10.20508/ijrer.v5i1.1868.g6481.

[13] A. Jouda, F. Elyes, R. Abdelhamid, and M. Abdelkader, "Simulation and real implementation of the fuzzy mppt algorithm for photovoltaic panel," *Indian Journal of Science and Technology*, vol. 10, pp. 1–11, 2017. DOI:10.17485/ijst/2017/v10i17/90437.

[14] H. Abid, A. Toumi, and M. Chaabane, "MPPT algorithm for photovoltaic panel based on augmented takagi-sugeno fuzzy model," *International Scholarly Research Notices*, vol. 2014, pp. 1–10, 2014. https://doi.org/10.1155/2014/253146.
[15] S. Abderrahim, M. Allouche, and M. Chaabane, "Intelligent power control of wind conversion system based on takagi–sugeno fuzzy model," *International Journal of Circuit Theory and Applications*, vol. 51, no. 5, pp. 2247–2265, 2023. https://doi.org/10.1002/cta.3517.
[16] M. Allouche, K. Dahech, M. Chaabane, and D. Mehdi, "T-S fuzzy control for mppt of photovoltaic pumping system," *Journal of intelligent & fuzzy systems*, vol. 34, no. 4, pp. 2521–2533, 2018.
[17] M. Allouche, K. Dahech, and M. Chaabane, "Multiobjective maximum power tracking control of photovoltaic systems: T-S fuzzy model-based approach," *Soft computing (Berlin, Germany)*, vol. 22, no. 7, pp. 2121–2132, 2018. https://doi.org/10.1007/s00500-017-2691-7.
[18] D. Ounnas, M. Ramdani, S. Chenikher, and T. Bouktir, "An efficient maximum power point tracking controller for photovoltaic systems using takagi–sugeno fuzzy models," *Arabian journal for science and engineering (2011)*, vol. 42, no. 12, pp. 4971–4982, 2017. https://doi.org/10.1007/s13369-017-2532-0.
[19] D. R. Lopez-Flores, J. L. Duran-Gomez, and J. Vega-Pineda, "Discrete-time adaptive pid current controller for wind boost converter," *IEEE Latin America Transactions*, vol. 21, no. 1, pp. 98–107, 2023. DOI:10.1109/TLA.2023.10015131.
[20] K. Ogata, *Sistemas de control en tiempo discreto*. Pearson Educación, 1996.
[21] S. Elert, "Programming possibilities using matlab simulink embedded coder on the example of data analysis from ahrs module," *Journal of Physics: Conference Series*, vol. 1507, p. 082042, mar 2020. DOI:10.1088/1742-6596/1507/8/082042.
[22] S. Stipa, A. Ajay, D. Allaerts, and J. Brinkerhoff, "Tosca – an open-source, finite-volume, large-eddy simulation (les) environment for wind farm flows," *Wind Energy Science*, vol. 9, no. 2, pp. 297–320, 2024. https://doi.org/10.5194/wes-9-297-2024.
[23] L. Legris, M. L. Pahus, T. Nishino, and E. Perez-Campos, "Prediction and mitigation of wind farm blockage losses considering mesoscale atmospheric response," *Energies*, vol. 16, no. 1, 2023. https://doi.org/10.3390/en16010386.

APPENDIX

TABLE IV
PARAMETERS OF THE SWT MODEL

Symbol	Parameter	Value
J	Inertia moment	1 Kg·m^2
ρ	Air density	1.225 Kg/m^3
R	Radius	2.9343 m
c_1, c_2, c_3		$5.953e^{-7}$, $-2.87e^{-5}$, 0.0005158
c_4, c_5, c_6	C_p constants	-0.004115, 0.01173, 0.005831
c_7, and c_8		0.01584, 0.004888

TABLE V
PARAMETERS OF THE PMSG GENERATOR

Symbol	Parameter	Value
R_s	Phase resistance	2.5 Ω
L_q, L_d	d-q inductances	6 mH
Ψ_m	Magnetic flux	0.5 v·s/rad
p	No. of poles	24

David R. López-Flores obtained a Master's degree of Science in Electronic Engineering in 2005 and a Doctor of Science degree in Electronic Engineering in 2022 from the Tecnológico Nacional de México / IT de Chihuahua Chih., México, where he is currently working as a full-time professor. He is interested in power electronic and mechatronic systems for conditioning renewable energies. Currently, he is a member of the National System of Researchers of the National Council of Humanities, Sciences, and Technologies in Mexico.

Pedro R. Acosta-Cano-de-los-Rios professor and researcher in the Automation and Industrial Informatics Group of the Graduate and Research Division of the Instituto Tecnológico de Chihuahua, Mexico. He received his Ph.D. degree from the Polytechnic University of Valencia, Spain in 2005. He is an Industrial Engineer in Electronics and a Master of Science in Electrical Engineering from the Instituto Tecnológico de Chihuahua. His current research interests are in the area of automatic control within the theory and application of control of nonlinear systems and, in particular, sliding mode control.

Pedro R. Márquez-Gutierrez received a degree in Industrial Engineering in Electronics from the Instituto Tecnológico de Chihuahua (TecNM/ITCH) México, a Master's degree in Computer Science from the Instituto de Investigaciones en Matemáticas Aplicadas y en Sistemas (IIMAS), Universidad Autónoma de México (UNAM), and a Ph.D. in Computer Science from New Mexico State University (NMSU), New Mexico, USA. He received the Chihuahua Prize in Science and Technology from the Government of the State of Chihuahua. He is a Research Professor at TecNM/ITCH. He has taught at NMSU, IIMAS-UNAM, UACJ, ITESM Campus Chihuahua, FEFyCD and FCA UACH, in different periods.

José E. Acosta-Cano-de-los-Rios was born in Chihuahua, México. He received his B.S. from Instituto Tecnológico de Chihuahua, a M.Sc degree from Case Institute of Technology and a Ph.D. from Universidad Politécnica de Madrid. His research interests concern supervisory control, flexible automation systems, and theorical aspects of automation. He has been as a titular professor at the Insituto Tecnológico de Chihuahua and Universidad Autónoma de Chihuahua.

Rogelio E. Baray-Arana received the BSc.(1987) and the MSc.(1990) degrees in electrical engineering from the Chihuahua Institute of Technology, Chihuahua, Chih., Mexico. Has been an research-professor with the Electrical-Electronics Engineering Department at Chihuahua Institute of Technology. His professional experience includes development of projects and consultancy for several companies. He currently works as a Research Professor at the Chihuahua Institute of Technology since 1991, in Chihuahua, Chih., Mexico where he is the director of the electromechanics control Laboratory and director of the Graduate Studies and Research Division. His research interests include mechatronic design, electronic power converter, control of electromechanical systems and robotics.

Graciela Ramírez-Alonso received the M.Sc. (2204) and Ph.D. (2015) degrees in EE from the Chihuahua Institute of Technology. She currently teaches in the undergraduate and graduate programs at the Universidad Autónoma de Chihuahua, Facultad de Ingeniería. She is currently a member of the National System of Researchers of the National Council of Humanities, Sciences and Technologies. Her research interests include computer vision, signal processing, fuzzy logic, and machine learning algorithms.